



# A study on vibration-suppression mechanism for risers using flexible structural joints

Tomo Fujiwara<sup>1</sup>

Received: 19 April 2023 / Accepted: 19 October 2023 / Published online: 2 January 2024  
© The Author(s) 2023

## Abstract

These new mechanisms for suppressing vibration in large diameter intake pipes and pumping systems has been developed for use in Floating Liquefied Natural Gas (FLNG) facilities. Like existing devices such as fairings and strakes, this mechanism is designed for practical use and has a flow path inside the pipe. The mechanism is designed to suppress vibration caused by both float motion and vortex-induced vibration (VIV) due to currents. Experiments were conducted using a scale model, and numerical calculations were used to evaluate the mechanism's ability to reduce vibration. As a result, the natural frequencies of the pipes were analyzed, and it was found that the vibration damping mechanism, when installed at appropriate locations, can provide effective vibration suppression against the motion of the upper float and vibration caused by VIV due to currents over the entire length of the pipe, even at limited installation locations. On the other hand, it was found that the vibration suppression effect could not be achieved without appropriate positioning, and that the longer the pipe length, the more limited the vibration damping capability.

**Keywords** Hanging pipe · VIV · Vibration control · Model experiment · Fluid–structure interaction · Underwater linear structures

## List of symbols

- OD Outer diameter of model pipe
- WO Cases without vibration-suppression mechanism installed
- DP Cases installed with damper-type vibration-suppression mechanism
- SP Cases installed with spring-loaded vibration-suppression mechanism
- LB Cases installed with laminated rubber vibration-suppression mechanism
- M4 Cases with suspension devices mounted at the 4-m arc length position

## 1 Introduction

Linear structures such as risers, intake pipes, and seabed mineral resource development systems have been used in off-shore development. Intake pipes are operated in suspension

in the sea without connection to the seabed. The SMS (sea-floor massive sulfide) lifting riser system is designed with a submersible pump suspended at the lower end of the system [1, 2]. Because the lower end is not fixed in the suspended condition, vibration may increase owing to the motion of the upper floating body, and vortex-induced vibration (VIV) in the current may increase. Similar problems arise with plant cooling-water intake pipes used in floating liquefied natural gas (FLNG) liquefaction and production facilities, where large-diameter pipes are suspended for operation [3]. Intake pipes were also used in the TAKUMI project, which used buoys to pump deep-ocean water for marine nutrient enhancement [4].

For underwater linear structures, the vibrations caused by the motion of the upper structure and currents can cause significant fatigue damage and are to be considered in the design. Thus, ball joints, bend stiffeners, and other mechanisms to reduce bending moments at the ends are often provided at the connection between the upper structure and the underwater linear structure. In addition, mechanisms such as a chain suspension of the connection to release the bending moment are used in suspension-type structures. Large-scale model tests of free-hanging intake pipes under vessel motion and model tests of top-end excitation and in-tidal VIV for

✉ Tomo Fujiwara  
tomo@m.mpat.go.jp

<sup>1</sup> National Maritime Research Institute, 6-38-1, Shinkawa, Mitaka, Tokyo 181-0004, Japan

three to five multi-intake pipes have also been conducted in previous studies [5–7]. Equipment such as strakes and fairings have been introduced worldwide as VIV-suppression devices. Strakes promote turbulence around the riser and prevent vortex shedding, fairings regulate the flow around the riser and make it less likely for vortex shedding to occur. With regard to strakes, evaluation through tank experiments using scale models, and behavior measurement and visualization experiments using wind tunnels have been conducted [8–11]. There are not as many papers on fairings as on helical strakes, but many studies have used tank experiments and computational fluid dynamics (CFD) [12]. There have been other studies on VIV control, including passive controls such as strakes and fairings with a viscoelastic layer around the pipe to increase damping, a proposal to install a mass damper on the outside of the pipe, and use of the inner pipe of a pipe-in-pipe as a mass damper [13–16]. In contrast, the vibration absorption mechanism investigated in this study is different from conventional VIV-suppression devices in that it is inserted into the joint between rigid risers.

The vibration modes caused by floating body motions are of a lower order than those caused by VIV; the lower end of the free boundary condition is always on antinode of the vibration. For example, in the case of two-node vibration, a node is created at approximately one-third of the length from the bottom, with an antinode at two-thirds of the length [17]. In general, the bending stresses are higher at the antinodes of vibration in linear structures; thus, the bending moments can be reduced by inserting joints that absorb bending at this point. For short-period vibrations such as VIV, effective vibration suppression can be achieved by inserting mechanical dampers. The deflections caused by VIV occurs at the top, where the current is faster. Thus, the VIV in a suspended pipe is more likely to break because the bending radius is smaller at the bottom owing to the lower tension, resulting in a greater bending stress, except at the top end or at specific points where there is a stress concentration.

In this study, a practical vibration-damping mechanism with a shape that does not disturb the flow path in the pipe was trial-designed for the afore-mentioned suspension riser system, with reference to existing riser joints and seismic isolation components in buildings. In addition, the behavior of a suspended riser system subjected to low-order modes and large-amplitude vibrations caused by floating body motions at the top end was measured in tank experiments using a scale model. The behavior of VIV caused by the riser being exposed to currents was also measured using a current generator. A behavior estimation model of the suspended riser system, including the vibration-suppression mechanism, was developed, compared, and verified with the measurement results. The effectiveness of the vibration-suppression mechanism against vibrations caused by the motion of the upper structure

in waves and VIV in currents was investigated through model tests and numerical calculations. Furthermore, as a case study, the effectiveness of the vibration-suppression mechanism was evaluated in a seabed mineral resource development system with and without the device.

## 2 Experimental approach

### 2.1 Design of vibration-suppression mechanism

The connection between the upper floating structure and the underwater linear structure is often fitted with a mechanism to reduce the bending moment at the end. This is a ball joint or bend stiffener, in which the connection is chain-suspended to release the bending moment [18]. Equipment such as strakes and fairings are often installed as VIV-restraint devices.

In the field of architecture, protecting buildings from earthquakes is critical. In addition to rigid construction of a structure, one method is seismic isolation, which is a method of absorbing the shaking of an earthquake. There are two main types of seismic isolation components: isolators that “parry” the shaking and dampers that “absorb” it. The respective classifications are shown in Table 1 [19].

When considering application of these seismic isolation components to suspended risers, the following three points are considered: (1) risers are under constant tension in the axial direction; thus, mechanisms such as sliding and rolling bearings, which are established by receiving loads, cannot be used; (2) deformations caused by earthquakes in structures are irregular and infrequent, whereas vibrations in risers are small and occur constantly; (3) vibrations in the vertical direction occur due to vertical movement of the upper floating structure.

Thus, in this study, it was assumed that a damping mechanism was installed at the joints of the risers; the following damping mechanisms were designed experimentally: The models of the damping mechanisms are illustrated in Fig. 1.

#### (i) Laminated rubber

**Table 1** Classification of seismic isolation components

Seismic isolation components	Isolators	Laminated rubber Plain bearings Rolling bearings
	Damper	Historical dampers Fluid dampers Viscoelastic dampers

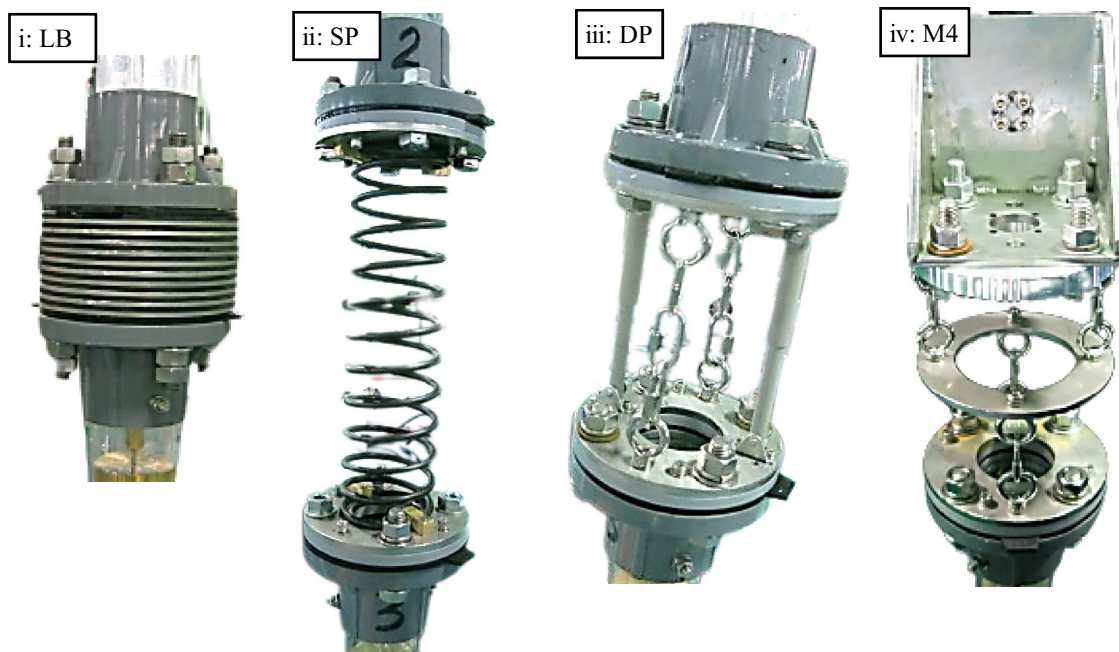


**Fig. 1** Vibration-suppression mechanism model: (i: laminated rubber; ii: spring; iii: damper; iv: suspension system)

The joints of the risers were connected by long bolts with alternating layers of steel and rubber plates between them to absorb the bending deformation of the pipe caused by rubber deformation. To make the rubber layer shear rigid to the scale of the model, a damping mechanism using a low-rebound urethane damping material was manufactured to match the scale of the model.

#### (ii) Spring

Springs were inserted between the links to absorb longitudinal vibration due to spring extension and to absorb bending stress due to shear deformation of the springs. The spring was selected to have a sufficiently high natural frequency in relation to the excitation and VIV frequencies to avoid resonance with the riser model.

#### (iii) Damper

The riser tubes were connected by two chains facing each other, and the fluid dampers were arranged in an orthogonal direction such that the dampers expand and contract when bending occur. In the model shown in Fig. 1, the transferred bending causes the fluid damper to expand and compress with a maximum stroke of 40 mm, dissipating energy as the oil inside passes through the orifice.

#### (iv) Suspension system

A mechanism that can absorb bending deformation in one direction due to the suspension chain is relayed by a ring and rotated in the orthogonal direction to combine with another one. This mechanism absorbs bending deformation

in all directions to release the bending moment generated at the connection with the floating body at the upper end [20].

## 2.2 Test facilities.

The model tests were conducted in the deep-sea basin of the National Maritime Research Institute, Japan. The basin was equipped with an optical behavior measuring device that enables non-contact measurement of the three-dimensional behavior of the model. A current generator capable of generating a maximum flow of approximately 0.35 m/s in the basin was also used to simulate the VIV of the riser model. An electric linear slider-forced excitation system was used to simulate the motion of the upper structure of the waves. The device was capable of excitation with constant and non-constant amplitude and period.

## 2.3 Riser system model

A 10-inch steel pipe riser was used as the basis for the assumed actual machine; the scale of the test model was approximately  $\lambda = 1/8$ . The relationship between the riser pipe model and the assumed actual machine is presented in Table 2. The weight of the model in air and in water was adjusted to be  $\lambda^2$  according to the law of geometric similarity, respectively, and the bending stiffness was adjusted to be  $\lambda^5$  to satisfy the law of dynamical similarity. On the other hand, the pipe diameter was set to 0.06 m without relying on the law of similarity to ensure a sufficient cross-sectional area to install the vibration control mechanism

**Table 2** Assumed actual equipment and model pumping pipe specifications

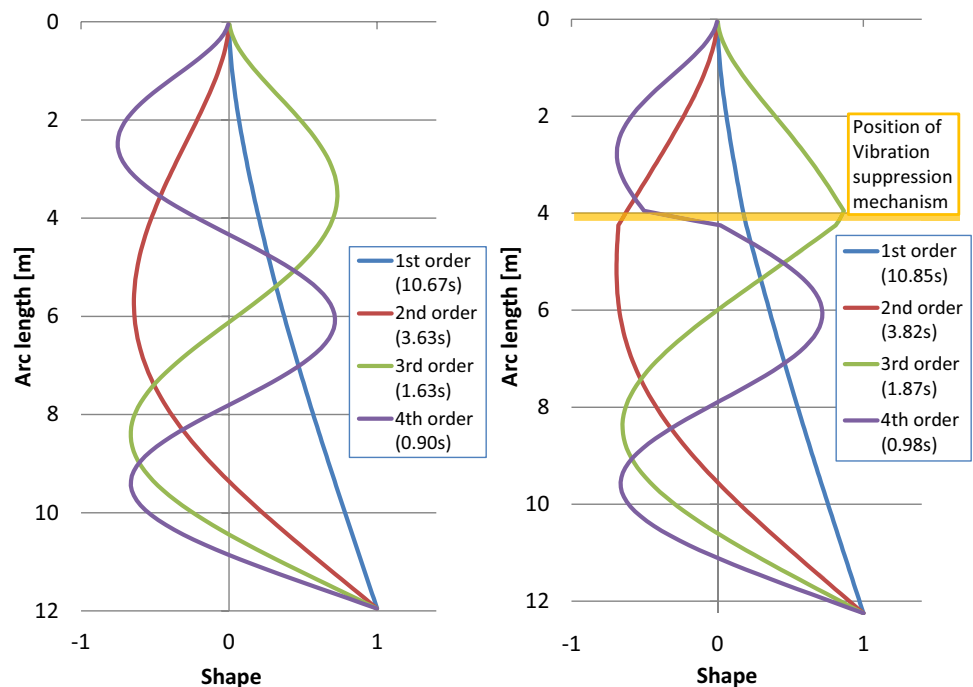
Item		Assumed actual equipment	Riser pipe scale model
Length	[m]	100	12.0
Outer diameter	[m]	0.254	0.060
<i>Bending rigidity</i>	<i>[Nm<sup>2</sup>]</i>	<i>2.49 × 10<sup>7</sup></i>	<i>395.9</i>
<i>Weight in air</i>	<i>[kgf/m]</i>	<i>143.7</i>	<i>2.38</i>
<i>Weight in water</i>	<i>[kgf/m]</i>	<i>124.9</i>	<i>1.88</i>

\*The model was designed to satisfy the similarity rule for the items in italics

model. This was approximately twice as large as  $\lambda$ . The riser model was constructed as one piece at 2 m, and six pieces were connected to form a scaled-down partial model with a total length of 12 m. The total length was shortened due to the limitations of the test facility. When the bending stiffness of the tube was measured using the three-point bending test, the bending stiffness of the laminated rubber and spring of the four vibration-suppression mechanism models were also measured. It was found that the laminated rubber type had 3.8% and the spring type had 0.3% of the pipe-model bending stiffness, indicating that the model had a discontinuity in bending stiffness as a vibration-suppression mechanism. The damper type and suspension system have structures that bend so easily that a three-point bending test is not possible, and they function as joints.

The natural frequencies of the riser system in this test were important for assessing the capability of the damping mechanism. Thus, eigenvalue analysis was performed prior to the test to determine the mounting position and excitation frequency of the vibration-control mechanism at the top end. Because the experimental model used in this study is long, eigenvalue analysis and modal analysis cannot be performed in air, where there is low damping by the fluid. Therefore, the eigenvalue analysis used the commercial software Orcaflex, which is widely used in the field of marine development as a finite element method (FEM) for behavior analysis of underwater linear structures such as riser systems. The results are shown in Fig. 2. The figure shows the first-order to fourth-order modes at the free end, with the left-hand figure showing the case without a vibration-suppression mechanism installed, and the right-hand figure showing the eigenvalue analysis results for the case with a vibration-suppression mechanism installed 4 m from the top end. The first-order to fourth-order modes at the free end of the model vibrated with eigen periods of 0.9–10.7 s. Attachment of the vibration-suppression mechanism caused a discontinuity between the bending stiffness and linear weight of the model, which increased the eigen period by approximately 0.1–0.2 s. On the actual scale, Global Wave Statistics are generally higher in the open sea by 4–10 s, which corresponds to 1.41–3.54 s in the scale of the model experiment. Thus, in this experiment, the capability of the vibration-suppression mechanism was verified mainly for the third-order mode at the free end, which corresponded to the actual wave period, based on the results of the eigenvalue analysis

**Fig. 2** Modal analysis results for riser (left) without and (right) with vibration-suppression mechanism



of the riser model. The vibration-suppression mechanism was installed at the flange connection with an arc length of approximately 4 m and had an antinode close to the upper end of the free-end third-order mode.

## 2.4 Test parameters

The arrangement of the model and equipment in the deep-sea basin is shown in Fig. 3. Measurements were taken for either a riser pipe model with no vibration-suppression mechanism or the four vibration-suppression mechanism models discussed in Sect. 2.3, each of which was attached to a joint 4 m from the top end. The behavior of the riser pipe and the forces and bending moments acting on the top end were measured using a six-component force transducer. Additionally, a suspension device was attached to the top end to release the bending moment, and measurements were taken at the fixed end without this device for comparison. The amplitude of the motion of the upper structure in waves varies. The main purpose of the upper end forced vibration test is to evaluate the effect of the motion frequency. Thus, the amplitude of the top end excitation was set to 1.0 m on the actual scale, and regular wave excitation was performed by changing the parameters with a vibration period corresponding to 4–16 s on the actual scale. In the current VIV

test, the pipe was subjected to a current equivalent to 5 knots in maximum on the actual scale. In the experiment, the outlet of the current generator was placed near the water surface to reproduce shallow surface currents. The average velocities presented in Table 3 correspond to 2 m below water surface (Table 3).

## 3 Numerical calculation

OrcaFlex from Orcina, which is widely used for predicting the behavior of underwater linear structures, was used for the numerical simulation in this study [21]. The conditions involved in the numerical analysis are shown in Table 4. The simulation model was simple, consisting only of a riser pipe and a vibration-suppression mechanism. The damping coefficients were calculated based on the results of hammering tests on a pipe model in air. The structural damping ratio of the riser model was quite high at 6.52%, which is attributed to the different vibrations of the outer plastic tube and the weight placed inside for weight adjustment. The damping coefficient of steel pipes used in offshore structures is generally considered to be approximately 0.5%, which means that the model used in this test is more likely to damp vibrations than the actual machine. The bending stiffness of the

**Fig. 3** Schematic of test setup

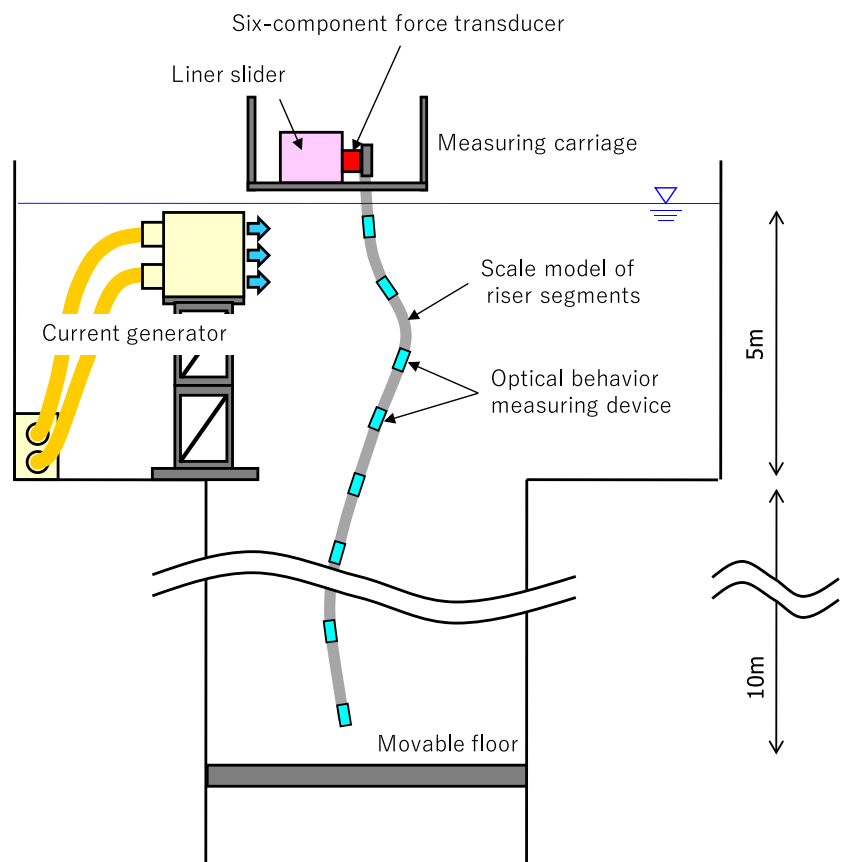


**Table 3** Test conditions

Parameters	Test conditions	Notes
Model	5 Cases in test (Without, vibration-suppression mechanism i, ii, iii, iv)	For the damper model, the mounting position was changed
Top-end forced oscillation	Vibration direction	Horizontal (1 axis)
	Vibration amplitude	0.12 m
	Vibration period	1.4–5.7 s
VIV in current	Flow velocity	0.05–0.30 m/s on average
	Flow direction	Horizontal

**Table 4** Calculation conditions for numerical analysis

Pipe length	12.0 m
Length of vibration-suppression mechanism	0.3 m
Element length	0.1 m
Fixing conditions at top end	Pin (with suspension device) Fix (without suspension device)
Fixing conditions at lower end	Free end
Damping factor of riser model	6.52% (Pipe)
Position of vibration-suppression mechanism	2m, 4m(default), 6m, 8m
Bending Stiffness of vibration-suppression mechanism model	1% of riser model
Damping force of vibration-suppression mechanism	Extended 60N Piston speed rate 0.04 m/s

vibration suppression mechanism was given as 1% of the riser model to prevent divergence of the calculations. In addition, damping force was set for the dampers of the vibration suppression mechanism with reference to the catalog specifications of the oil dampers that are the components of the model. The damping force of an oil damper acts only in the extension direction, but since two oil dampers are used in the model, the damping force is equal for both bending regardless of the direction of excitation.

## 4 Results

### 4.1 Model experiment

As an example of the results of the top-end forced vibration test, a comparison of the amplitude distribution is shown in Fig. 4. For a vibration period of 5.65 s, which was close to the free-end second-order mode, a vibration period of 3.53 s, which was close to the free-end third-order mode, and a vibration period of 1.53 s, which was close to the free-end fourth-order mode. These three vibration periods correspond to 16.0 s, 10.0 s, and 4.3 s, respectively, in the actual equipment. The amplitudes were made dimensionless by dividing them by the upper end excitation amplitudes. There was little difference in amplitude between cases without

a vibration-suppression mechanism. There are likely two reasons: (1) the free-end second-order mode vibration was relatively slow; thus, the vibration-suppression mechanism model moved in unison without bending; (2) in the free-end third-order mode, the mounting position of the vibration-suppression mechanism model fell between the antinode and node of the vibration; thus, vibration suppression could not be demonstrated. In contrast, the vibration-suppression mechanism exhibited the best performance at a vibration period of 1.53 s. The amplitude was reduced at the position where the vibration-suppression mechanism was installed at the other antinode and free end. In a regularly vibrating underwater linear structure, the bending stress fluctuations are the highest at the vibration antinode; thus, reducing the amplitude at this position is important to the integrity of the entire system.

A comparison of the amplitudes at the antinode position of the free-end second- to fourth-order vibration modes generated at each excitation period is shown in Fig. 5. In terms of the arc length, the amplitudes were approximately 4 m, 6 m, and 8 m, respectively. The results show that the vibration-suppression mechanism had no effect on the amplitude of the free-end second-order and third-order modes. The amplitude of the free-end fourth-order mode was reduced, especially at the position of the vibration antinode; the damper type produced the largest reduction

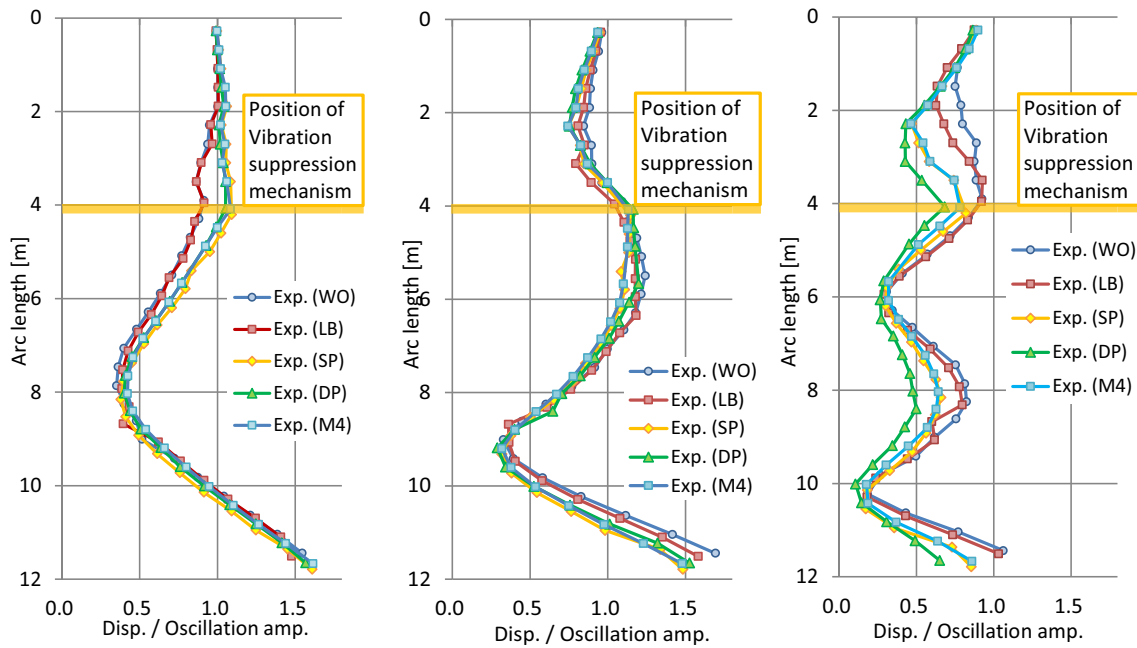


**Fig. 4** Top-end forced vibration test results (top oscillation amplitude 0.06 m, left figure: vibration period 5.65 s, middle figure: 3.53 s, right figure: 1.53 s)

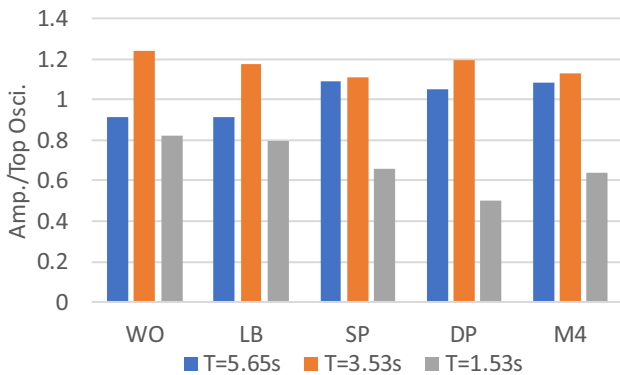


**Fig. 5** Comparison of amplitudes at antinode position for each vibration mode, the position of the vibration suppression mechanism is 4.0 m at  $T=5.65$  s, 5.5 m at  $T=3.53$  s, and 8.3 m at  $T=1.53$  s

in amplitude (up to 40%) compared to the amplitude without the vibration-suppression mechanism. The damping force provided by the fluid damper vibration-suppression mechanism model was the most effective in reducing the amplitude. The suspension and spring vibration-suppression mechanisms did not generate a damping force; thus, simply releasing the bending moment created a state in which the free-end fourth-order mode vibration was connected by a joint between the two tubes at the upper 4 m and lower 8 m, which shifted the natural frequencies. The laminated rubber system had a higher bending rigidity than the other models; thus, the vibration suppression

effect was weaker. Although detailed tuning was not performed in this test, this method is also used in existing flexible joints in terms of damping force and durability, so it is likely that a higher effect could have been obtained by approaching the design based on the specifications of existing equipment would have been more effective in the model test.

The measurement results for VIV behavior in the currents are shown in Fig. 6. The figure shows two cases without a vibration-suppression mechanism installed, where VIV was observed at flow velocities of 0.2 m/s and 0.3 m/s. The figure also shows four cases with an installed vibration-suppression mechanism, measured under the same conditions. The amplitudes were made dimensionless by dividing them by the outer diameter of the pipe model. The results without the vibration-suppression mechanism show that with 0.2 m/s and 0.3 m/s flow velocity, the current from the surface to a depth of 2 m travels the VIV to the lower end position of the 12 m length. The amplitude also increased with the mean flow velocity; however, the generated vibration modes were free-end third-order modes in both cases. Comparing the amplitude distributions with and without the vibration-suppression mechanism, the VIV amplitude increased over the entire length of the model when no vibration-suppression mechanism was installed. The amplitudes at the antinode and lower end decreased in the following order: laminated rubber, suspension, spring, and damper, indicating that the vibration-suppression mechanism with damping exhibited better vibration suppression.

**Fig. 6** Results of VIV measurements in currents (left: mean velocity 0.2 m/s, right: mean velocity 0.3 m/s)

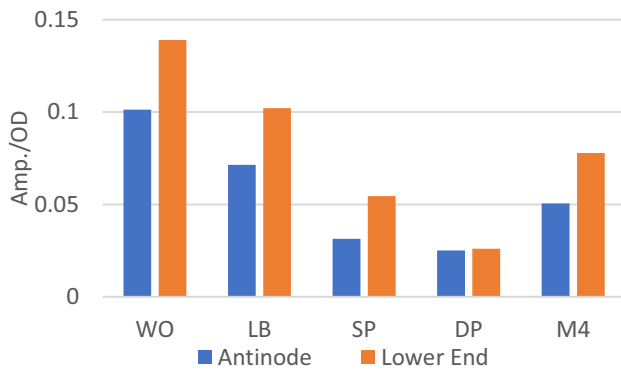
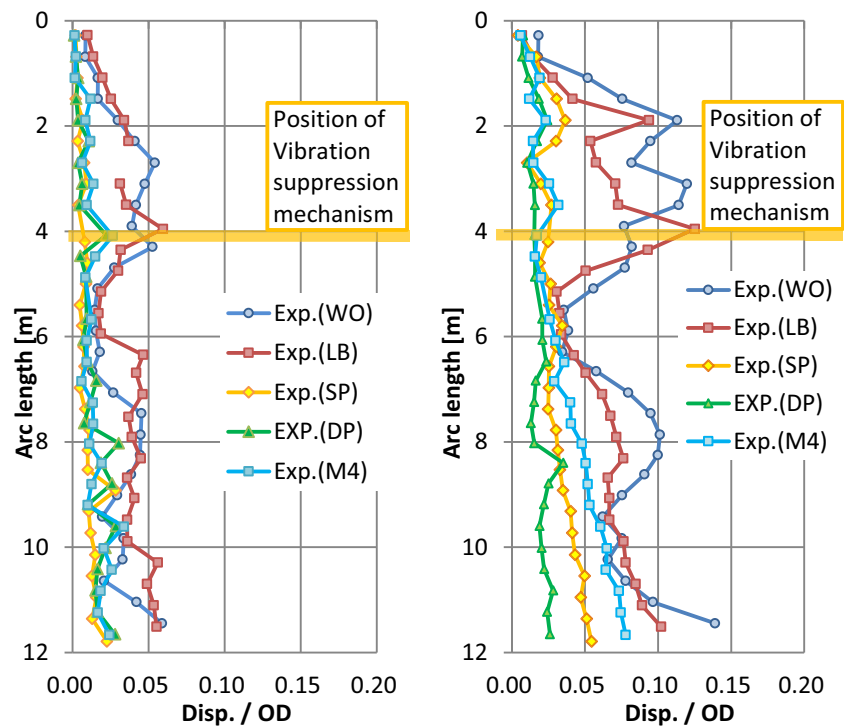


**Fig. 7** Comparison of amplitudes at the two lower-end antinodes in mean velocity 0.3 m/s, the position of the vibration suppression mechanism is 8.0 m at antinode and 11.6 m at lower end

The vibration-suppression mechanism was installed at an arc length of 4 m from the top end, which is close to the vibration mode antinode, and reduced the vibration. However, amplitude reduction also occurred at an arc length of 8 m and at the bottom end, where there was no vibration-suppression mechanism. A comparison of the amplitudes of the two lower end antinodes is shown in Fig. 7. It was found that the amplitude reduction was stronger than the forced oscillation at the upper end, with a 27–81% reduction in the vibration caused by VIV.

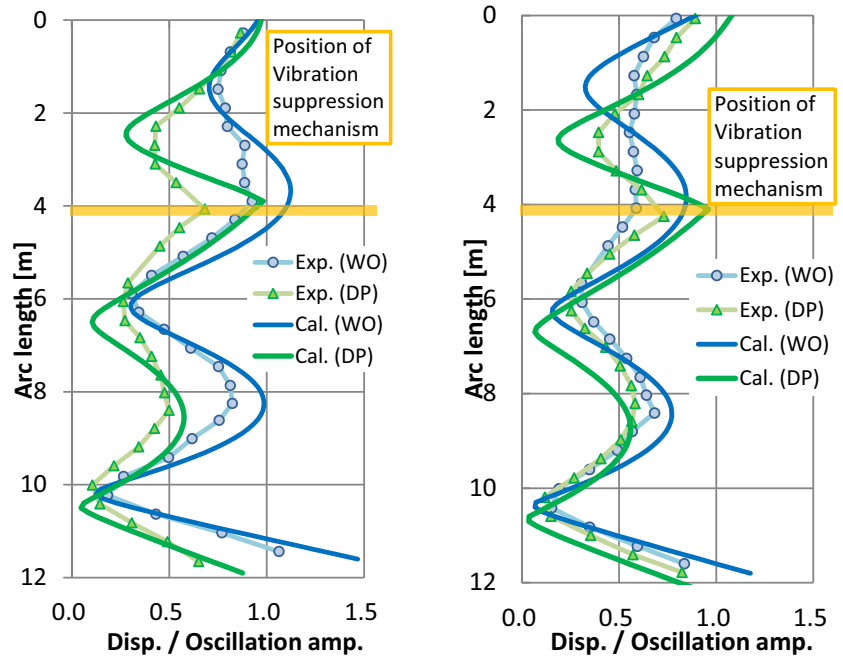
## 4.2 Comparison with numerical results

A comparison of the amplitude distributions of the numerical simulation results under the calculation conditions corresponding to the model test is shown in Fig. 8. The symbols indicate the experimental results and the lines indicate the numerical simulation results. The oscillation period was set to  $T = 1.53$  s, which corresponded to the fourth-order mode at the free end, where the performance of the vibration-suppression mechanism was best demonstrated. The left figure shows the same top-end fixed case as that in the top-end excitation experiment shown in Fig. 2; the right figure shows the results with a pin support using a suspension device at the top end. The cases fitted with vibration-suppression mechanisms are shown in the figures as representatives of the damper type, which had the highest vibration suppression capacity. The models for the numerical simulations were created according to the specifications of the damper-type (DP in legend) vibration-suppression mechanism used in the experiments. It will of course be important to evaluate the damping performance in the process of optimizing the damping mechanism, since changing the damper's capacity could change its effect on the response.

Approximate agreement was obtained between the model tests and numerical simulations for the cases without a vibration-suppression mechanism with a fixed top end and a damper-type vibration-suppression mechanism. An approximate agreement of the amplitude distribution was also obtained when the upper end was free from the



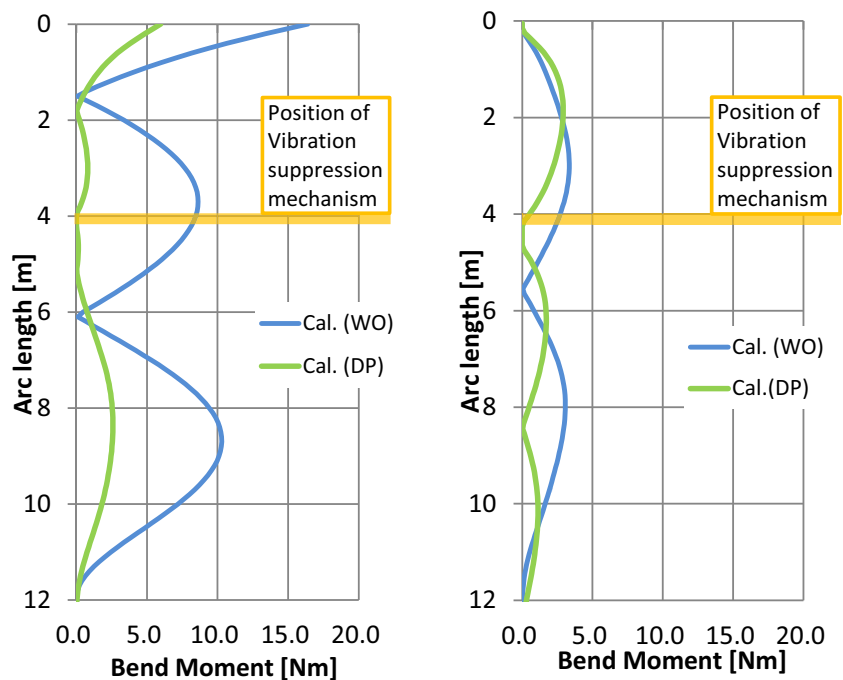
**Fig. 8** Comparison of amplitude distribution in model test and numerical simulation (left: fixed support at top end, right: pin support at top end)



bending moment by attaching a suspension device. From these results, it was concluded that the model used in the numerical simulation correctly modeled the experiment. The bending moment, which was difficult to measure at the targeted position in the model experiment, was evaluated. The results are shown in Fig. 9. Comparison of the bending moment distribution in the numerical simulation shows that in the case of a fixed top end, the bending moment was reduced at the position where the vibration-suppression

mechanism was installed, as well as over the entire length of the pipe and at the lower end and upper end connection points. Furthermore, in the case of the free bending moment at the top end, the vibration-suppression mechanism had a moment reduction effect, especially from the vibration-suppression mechanism installed at the bottom end of the pipe, although the bending moment reduction effect was not as significant as that at the fixed top end.

**Fig. 9** Distribution of bending moments (left: top-end fixed support; right, top-end pin support)



A numerical parameter study was conducted to verify the effect of different vibration-suppression mechanism mounting positions on the bending moment reduction. In Fig. 10, the upper figure shows the maximum amplitude, and the bottom figure shows the maximum bending moment. The figure shows a case with the vibration-suppression mechanism installed at an arc length of 4 m from the top, the same position as in the tank test, a case with the vibration-suppression mechanism installed at an arc length of 2 m near the top, a case with an arc length of 6 m in the middle of the entire riser model, a case with an arc length of 8 m near the bottom, and a case without the vibration-suppression mechanism. The upper end was fixed, and the maximum bending moment at the antinode, excluding the upper end, was considered as the representative value for each excitation period. In the case where the vibration-suppression mechanism was not installed, the maximum bending moment increased at a vibration period of 1.6–1.8 s, which corresponds to approximately 5 s in the actual machine, and at a vibration period of 3.5 s, which corresponds to approximately 10 s in the actual machine. The two peaks corresponded to the eigen period of the free-end fourth-order mode and free-end third-order modes, respectively, and the amplitude and bending moment increased due to the resonance. In contrast, when the vibration-suppression mechanism was installed 4 m from

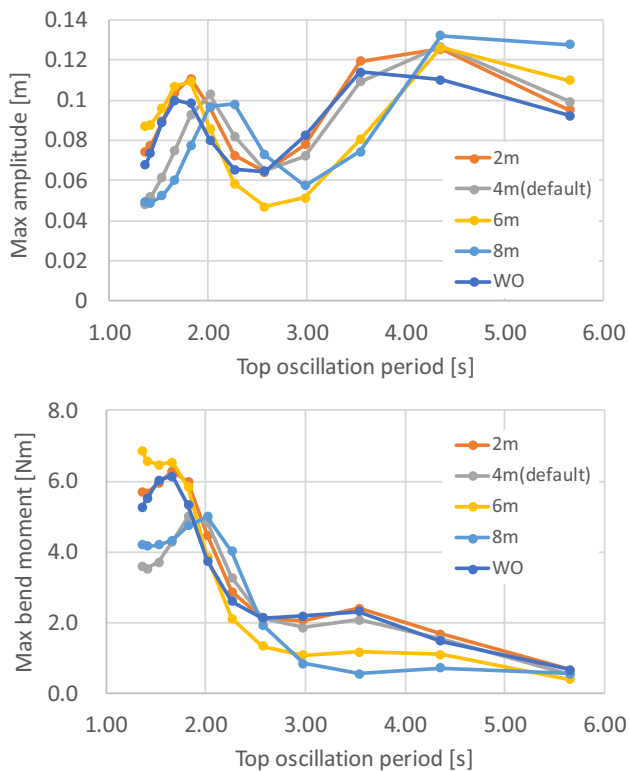


**Fig. 10** Effect of vibration-suppression mechanism mounting position (upper: maximum amplitude, bottom: maximum bending moment)

the top end, it was installed at one of the antinodes of the third-order vibration, thereby reducing the bending moment generated by this vibration mode. For the same reason, the bending moment was also reduced in the case where the damping mechanism was installed at the 8 m arc length. With the vibration-suppression mechanism installed at arc lengths of 6 m and 8 m, the bending moment generated by the two-node vibration was suppressed at periods longer than 2.5 s, compared with the case without the vibration-suppression mechanism. However, the maximum amplitude was larger than that in the case without the vibration-suppression mechanism, particularly for long vibration periods, and the effect of the lower-end swing may be stronger. In addition, the maximum values of the amplitude and bending moment for arc lengths of 2 m and 6 m were higher than those without the vibration-suppression mechanism with short vibration periods. Thus, it is important to analyze the natural frequencies of pipes and consider the installation position when suppressing the vibrations caused by wave motions with a vibration-suppression mechanism.

### 4.3 Case study for actual scale

A case study was conducted with use of the vibration-suppression mechanism in an actual system. The assumed actual machine was a hang-off pipe connected to the upper structure; it was a 10-inch steel pipe, as assumed in the model test. The pipe lengths were 100 m, 200 m, and 400 m, and the effects of the presence or absence of vibration-suppression mechanisms were evaluated in terms of the amplitude and bending moment. The upper structure was set to move only in the horizontal and vertical directions and the upper end was set to follow the wave position regardless of the wave period. The upper end of the pipe was pin-supported to allow the bending moment to be free, assuming actual operating conditions. The vibration-suppression mechanism was installed at the position where the bending moment was maximum based on the results without the vibration-suppression mechanism, which in this study was approximately an arc length of 15 m from top-end. The calculations for the six cases are shown in Figs. 11 and 12, which show the distributions of the motion amplitude and bending moment, respectively. The left figure shows the JONSWAP spectrum with  $H_s = 10$  m and  $T_z = 13.75$  s as the long-period irregular wave motion, and the right figure shows the results for  $H_s = 7$  m and  $T_z = 8$  s as the short-period irregular wave motion. For the vertical axis in the figure, the position was made dimensionless by dividing by the arc length according to the different arc lengths of the models.

The vibration-suppression mechanism reduced the vibration amplitude over the entire length of the pipe for a total length of 100 m. However, no reduction in the vibration amplitude was observed for a total length of 200 m or

**Fig. 11** Distribution of amplitudes during top-end excitation with irregular waves (left:  $H_s=10$  m,  $T_z=13.75$  s; right:  $H_s=7$  m,  $T_z=8$  s)

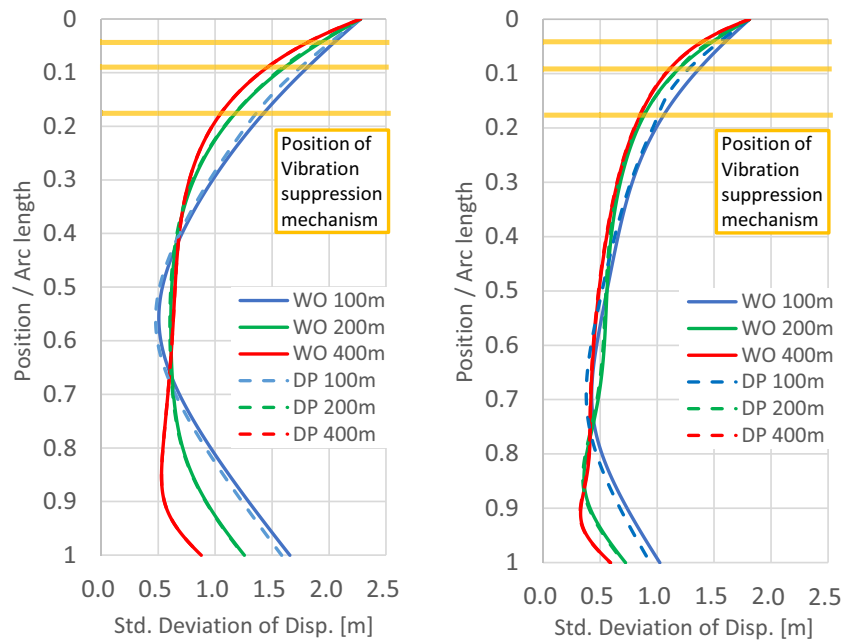
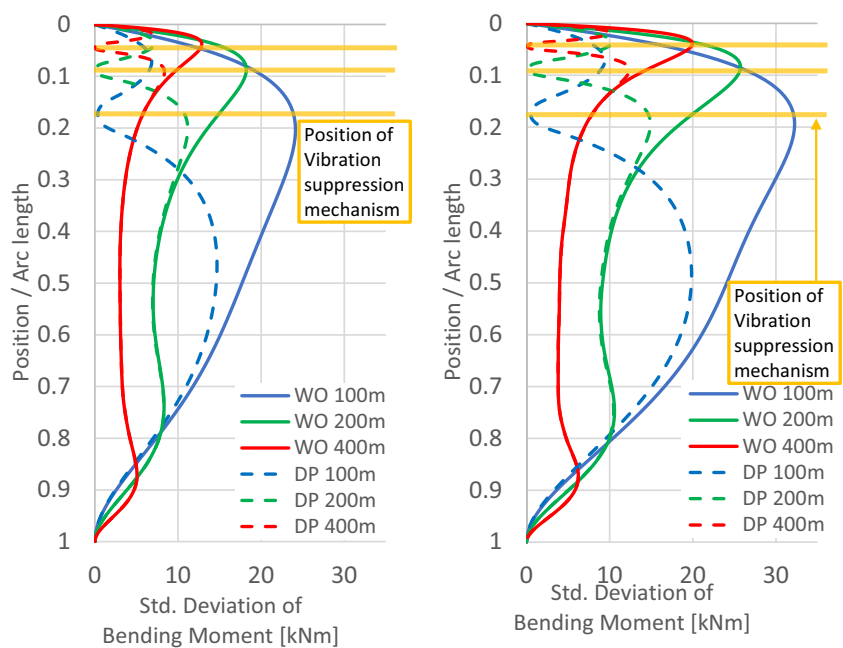


**Fig. 12** Distribution of bending moments during top-end excitation with irregular waves (left:  $H_s=10$  m,  $T_z=13.75$  s; right:  $H_s=7$  m,  $T_z=8$  s)



more. This was attributed to the increased weight of the pipe, which generated a large tension in the vibration-suppression mechanism installed near the top end, making it difficult to bend. Thus, the mechanism behaved in the same way as the pipe section. Based on the bending moment distribution, the bending moment received by the pipe was reduced by installing a vibration-suppression mechanism at the position where the bending moment was concentrated. Furthermore, with a 100-m length, the bending moment distribution was also reduced below the position

where the vibration-suppression mechanism was installed. However, the effect of the vibration-suppression mechanism was localized in cases where the total length was 200 m or more. Although it is possible to install multiple suppression mechanisms, the effect of the second and later mechanisms would be limited, since the most effective is to install them at points where the amplitude is large. It is also necessary to consider that this would complicate the system and increase costs.

## 5 Discussion

Based on the results of the experiments and numerical simulations, the advantages and disadvantages of fabricating and installing a vibration-suppression mechanism in an actual machine compared to existing VIV suppression devices such as strakes and fairings can be summarized as follows:

### Advantages

- Vibration-suppression mechanisms can be installed at appropriate installation positions based on analysis of the natural frequencies of the pipes, providing vibration suppression capabilities over the entire length of the system
- Limited installation positions
- Effective against vibrations caused by upper float motion and VIV in currents
- Low drag increase
- Disadvantages
- Can only provide vibration suppression if properly positioned
- Durability is required due to the concentration of bending in the system
- Vibration damping capacity is limited as the overall length of the pipe increases

Responses to the disadvantages will not be a problem, as information on suitable installation locations will be available from information from the fundamental analysis carried out for all projects. It may be more difficult and costly to design and manufacture a vibration-suppression mechanism that is more durable and flexible than a pipe; however, this can be addressed using existing applications in marine engineering, such as flexible joints. Even if the vibration damping capacity is limited, with a greater overall pipe length, vibration suppression at the most critical points of the system is achievable. In addition, comparison with methods that have many applications, such as fairings and strakes, is necessary for evaluation. This paper considers the vibration control mechanism concept as a first step in this process. On the way to optimizing the vibration suppression mechanism, it will be necessary to evaluate the advantages and disadvantages of this mechanism, including comparisons of vibration suppression capability, cost, safety, etc. The study in this paper was not sufficient to demonstrate the effectiveness of the proposed system against currents. In future research, it is planned to study the effect of the mounting position of the vibration suppression mechanism on VIV in currents and to use a numerical simulation model to study the effect of this mechanism.

## 6 Conclusions

A vibration-suppression mechanism, unlike existing VIV-suppression devices such as strakes and fairings, was trial-designed. It targets a large-diameter intake pipe for the FLNG or a pipe with a layout suspended from the upper floating structure in the pumping system used in the SMS development. Experiments using a scale model and numerical calculations were conducted to evaluate the ability to suppress vibrations caused by upper floating-body motions and the VIV caused by currents. The results showed that the vibration amplitude and bending moment reduction at the antinode were effective for vibrations close to the targeted natural vibration modes for top-end excitation. It was also shown to have a vibration damping capability against VIV in currents. Parametric studies were conducted on the installation position of the vibration-suppression mechanism and the length of the adaptable hanging pipe. The results showed that changing the installation position can damp the top-end oscillations with different vibration modes; however, other vibration modes may produce no bending moment reduction or swinging near the bottom end. It was also shown that the vibration and bending moment reduction over the entire length of the tube confirmed in the model tests became localized when the total length of the pipe was increased.

**Acknowledgements** The authors thank S. Kanada for technical assistance with the experiments. This study was supported by the JSPS KAKENHI (Grant number: JP 26630461).

**Open Access** This article is licensed under a Creative Commons Attribution 4.0 International License, which permits use, sharing, adaptation, distribution and reproduction in any medium or format, as long as you give appropriate credit to the original author(s) and the source, provide a link to the Creative Commons licence, and indicate if changes were made. The images or other third party material in this article are included in the article's Creative Commons licence, unless indicated otherwise in a credit line to the material. If material is not included in the article's Creative Commons licence and your intended use is not permitted by statutory regulation or exceeds the permitted use, you will need to obtain permission directly from the copyright holder. To view a copy of this licence, visit <http://creativecommons.org/licenses/by/4.0/>.

## References

1. Leach S, Smith G, Berndt R (2012) SME Special Session: Subsea Slurry Lift Pump Technology-SMS Development. In: Offshore Technology Conference. Presented at the Offshore Technology Conference, Offshore Technology Conference, Houston, Texas, USA. <https://doi.org/10.4043/23224-MS>
2. METI, Mining, Advisory Committee on SMS, JOGMEC (2013) Final Report of SMS Development Program Stage 1.
3. Shell (2009) Shell Prelude FLNG Project.
4. Ouchi K (2009) Results From Real Sea Experiment of Ocean Nutrient Enhancer TAKUMI, In: Ocean Engineering; Ocean

- Renewable Energy; Ocean Space Utilization, Parts A and B, vol 4 Presented at the ASME 2009 28th International Conference on Ocean, Offshore and Arctic Engineering, ASMEDC, Honolulu, Hawaii, USA, pp. 1473–1480. <https://doi.org/10.1115/OMAE2009-79866>
5. Fujiwara T, Masanobu S, Shimizu K (2013a) A Study of the Elastic Response of a Multi-line Riser System, the 1st Report -Experimental Study of an Effect of Top-end Oscillation-, Conference Proceedings The Japan Society of Naval Architects and Ocean Engineerings, vol 16, pp 267–270
  6. Fujiwara T, Masanobu S, Shimizu K (2013b) A Study of the Elastic Response of a Multi-line Riser System, the 2nd Report -Investigation about and Effect of VIV-, Conference Proceedings The Japan Society of Naval Architects and Ocean Engineerings, vol 16, pp 271–274
  7. Wang J, Xiang S, Fu S, Cao P, Yang J, He J (2016) Experimental investigation on the dynamic responses of a free-hanging water intake riser under vessel motion. *Mar Struct* 50:1–19. <https://doi.org/10.1016/j.marstruc.2016.06.003>
  8. Baarholm GS, Martin Larsen C, Lie H (2005) Reduction of VIV using suppression devices—An empirical approach. *Mar Struct* 18:489–510. <https://doi.org/10.1016/j.marstruc.2006.01.003>
  9. Gao Y, Yang J, Xiong Y, Wang M, Peng G (2016) Experimental investigation of the effects of the coverage of helical strakes on the vortex-induced vibration response of a flexible riser. *Appl Ocean Res* 59:53–64. <https://doi.org/10.1016/j.apor.2016.03.016>
  10. Simantiras P, Willis N (1999) Investigation on vortex induced oscillations and helical strakes effectiveness at very high incidence angles. In: Proceedings of the International Offshore and Polar Engineering Conference, Brest, France
  11. Zhou T, Razali SFM, Hao Z, Cheng L (2011) On the study of vortex-induced vibration of a cylinder with helical strakes. *J Fluids Struct* 27:903–917. <https://doi.org/10.1016/j.jfluidstructs.2011.04.014>
  12. Baarholm R, Skaugset K, Lie H, Braaten H (2015) Experimental Studies of Hydrodynamic Properties and Screening of Riser Fairing Concepts for Deep Water Applications. In: CFD and VIV, vol 2. Presented at the ASME 2015 34th International Conference on Ocean, Offshore and Arctic Engineering, American Society of Mechanical Engineers, St. John's, Newfoundland, Canada, p. V002T08A054. <https://doi.org/10.1115/OMAE2015-41730>
  13. Borges FCL, Roitman N, Magluta C, Castello DA, Franciss R (2014) A concept to reduce vibrations in steel catenary risers by the use of viscoelastic materials. *Ocean Eng* 77:1–11. <https://doi.org/10.1016/j.oceaneng.2013.12.004>
  14. Hong K-S, Shah UH (2018) Vortex-induced vibrations and control of marine risers: a review. *Ocean Eng* 152:300–315. <https://doi.org/10.1016/j.oceaneng.2018.01.086>
  15. Nikoo HM, Bi K, Hao H, n.d. (2017) Passive Vibration Control of Pipe-in-pipe (PIP) Systems Subjected to Vortex Induced Vibration (VIV). The 27th International Ocean and Polar Engineering Conference, San Francisco, California, USA
  16. Song J, Wang T, Chen W, Guo S, Yan D (2020) Vibration control of marine top tensioned riser with a single tuned mass damper. *JMSE* 8:785. <https://doi.org/10.3390/jmse8100785>
  17. Nakagawa K, Murotsu Y, Iwatsubo T (1998) Industrial vibration Science, 2nd edn. MORIKITA PUBLISHING, Tōkyō
  18. Cox AJ, Efthymiou M (2008) Water Intake Riser. United States Patent and Trademark Office, USA, Patent No. US 7.451,716 B2. Online at <https://patentimages.storage.googleapis.com/41/b4/ec/f1ec42b6d93609/US7451716.pdf>. Accessed 2 Nov 2023
  19. Nihon M, Kōzō K (eds) (2010) Menshin kōzō: buzai no kihon kara sekkei. In: Dai 1-han (ed) sekō made, Ōmusha, Tōkyō
  20. Takahashi I (2010) Riser tube suspension device and mooring tube coupling device. Online at. <https://www.j-platpat.inpit.go.jp/c1800/PU/JP-5665024/7602A6A835860B71D262C6476285389DC3D92F31AE39426480F8E64F62573941/15/en>. Accessed 28 Dec 2023
  21. Orcaflex O (2012) Online at. <https://www.orcina.com/orcaflex/>. OrcaFlex. Pdf. Access date 2 Nov 2023

**Publisher's Note** Springer Nature remains neutral with regard to jurisdictional claims in published maps and institutional affiliations.